D. J. DiMaria D. R. Young W. R. Hunter C. M. Serrano

Location of Trapped Charge in Aluminum-Implanted SiO₂

Abstract: The position of the centroid of electrons trapped on sites resulting from aluminum implantation into SiO₂ is measured by using the photo *I-V* technique for energies from 15-40 keV, oxide thicknesses from 49-140 nm, and post-implant annealing temperatures from 600-1050°C in N₂ for 30 min. The centroid of the trapped electrons is found to be identical to that of the implanted aluminum from SIMS measurements, regardless of annealing temperature from 600 to 1050°C, and located closer (by less than 9 nm) to the Al-SiO₂ interface than predicted from the Lindhard-Scharff-Schøtt (LSS) calculations of Gibbons, Johnson, and Mylroie. Comparison of centroids determined from photo *I-V* and SIMS measurements as a function of SiO₂ thickness also implies that the distributions of the ions and negative trapped charge are the same. The trapping behavior of these sites is discussed in the accompanying paper by Young et al.

Introduction

An understanding of the electron trapping behavior of SiO₂ implanted with Al requires information concerning the spatial distribution of the traps as compared with that of the implanted ions. Previous investigators (Johnson et al. [1]) using metal/silicon dioxide/silicon (MOS) structures had observed a discrepancy between the profiles, with the trapped electrons being located closer to the Si-SiO₂ interface than the implanted ions. Their measurements indicated that this discrepancy was due to a large trap density that resulted in complete trapping of all the injected electrons before they reached the location of maximum trap concentration. To overcome this difficulty, we have reduced the fluence of the implanted ions from 1×10^{14} Al ions/cm² to 1×10^{13} Al ions/cm², and we have annealed our samples at temperatures up to 1050°C. The annealing procedure removes most of the atomic displacement damage, and thus we expect our measurements to be dominated by the effect of the Al. For our case, the electron capture probability (defined as the product of the capture cross section and the number of empty traps per unit area) was reduced to about 10^{-3} (one out of every thousand injected electrons gets trapped) as compared with 1 (every injected electron gets trapped) in the previous work cited.

The experimental technique used by Johnson et al. [1] is somewhat similar to that of Yun [2, 3] in that it relies on every electron injected from the Si-SiO_o interface being trapped in the SiO_a layer. This is a severe restriction. Under these conditions the centroid is found closer to the injecting interface [2-4]. The use of a trapping region with low capture probability requires a different method for locating trapped charge. The photocurrent-voltage (photo I-V) technique developed by DiMaria [5], which does not have the restriction of Yun's technique, is used here for locating the centroid of negative trapped charge in the silicon dioxide layer. Until recently, the capacitance-voltage (C-V) technique [6] was used exclusively to determine the product of the centroid position and the total trapped charge per unit area in the oxide layer. The photo I-V technique allows determination of both the centroid and the total trapped charge and not just their product. The photo I-V technique is particularly sensitive to trapped charge located in the oxide bulk as opposed to very near an interface [5, 7].

Copyright 1978 by International Business Machines Corporation. Copying is permitted without payment of royalty provided that (1) each reproduction is done without alteration and (2) the *Journal* reference and IBM copyright notice are included on the first page. The title and abstract may be used without further permission in computer-based and other information-service systems. Permission to *republish* other excerpts should be obtained from the Editor.

289

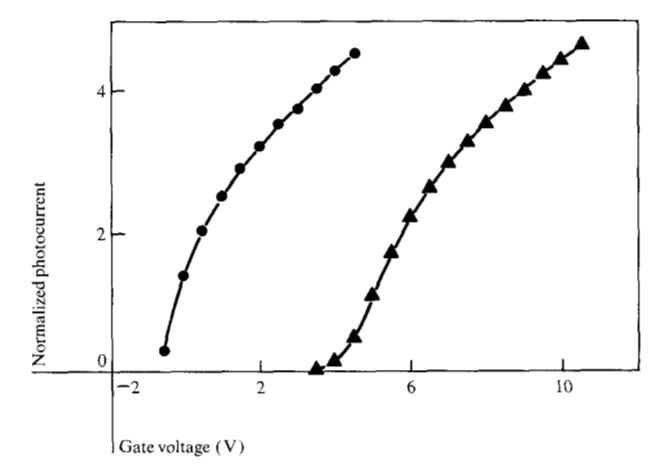


Figure 1 Normalized photocurrent (photocurrent divided by area and light intensity) for 5-eV radiation as a function of positive gate voltage (Si injecting): —control, —charged by electron avalanche injection from the Si substrate. The MOS structure had a SiO₂ layer 140 nm thick, 20-keV and 1×10^{13} Al/cm² implant, and was annealed at 1050° C for 30 min in N₂ after implantation prior to metallization. The average photo *I-V* voltage shift for positive gate polarity ΔV_{π}^{+} is 5.34 ± 0.06 V.

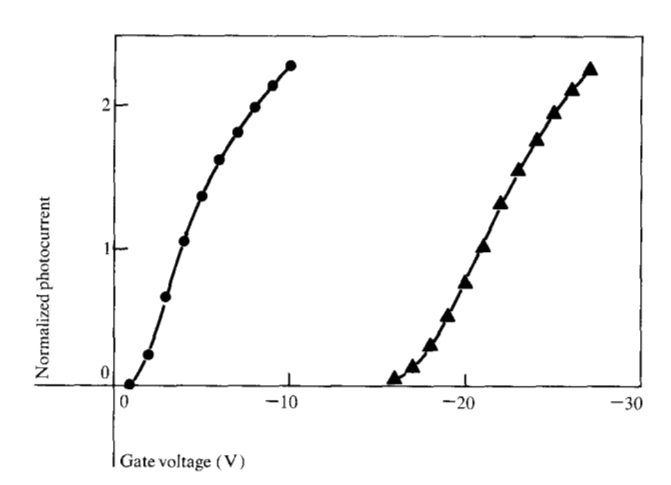


Figure 2 Normalized photocurrent for 4.5-eV light as a function of negative gate voltage (Al injecting). Samples are the same as in Fig. 1. The average photo I-V voltage shift for negative gate polarity $\Delta V_{\rm g}^-$ is -17.23 ± 0.11 V.

Experiment

• Sample preparation

The sample preparation is discussed in the accompanying paper by Young et al. [8]. The MOS structures had SiO₂ thicknesses of 49, 73, and 140 nm. Implantation energies of 15, 20, 30, and 40 keV and post-implantation annealing conditions from 600 to 1050°C in N₂ for 30 min were used.

However, in this study only thin (10-15-nm) Al electrodes were used to allow penetration of the incident light through the Al into the Si substrate so that internal photoemission currents (on which the photo *I-V* technique is based) were generated. All oxide thicknesses were measured by ellipsometry.

Measurement technique

The Al-implanted MOS structures are in approximately a net neutral charge state after the processing. To use the photo *I-V* technique, which depends on the presence of internal fields created by trapped charge in the insulator, the traps in the SiO₂ layer must be charged. This is accomplished by avalanche injection from the Si substrate [9] or by internal photoemission from either the Si or semitransparent metal contacts [10]. As described in [8], some of these injected electrons are trapped on sites related to the implanted Al. Without the implanted Al, no noticeable electron trapping is seen under similar injection conditions [11].

The photo I-V technique has been discussed in detail in recent publications [5, 12-14], and only the principal features and their application to this study will be discussed here. The technique is nondestructive and has a sensitivity of less than 10¹¹ trapped charges/cm². The experimental setup for the photo I-V measurements has been reported elsewhere [15]. Figures 1 and 2 show typical photo I-V data for both gate voltage polarities on a control (uncharged) and a charged MOS structure, each fabricated on a 140-nm SiO₃ layer implanted with a fluence of 1 \times 10¹³ Al/cm² at 20 keV and annealed at 1050°C in N₂ for 30 min after implantation prior to metallization. From the parallel voltage shifts for positive gate bias $\Delta V_{
m g}^+$ and for negative gate bias ΔV_g^- between the *I-V* curves in Figs. 1 and 2, the centroid \bar{x} measured from the metal-oxide interface and the number of trapped charges per unit area Q/e were determined from the photo I-V relations [5] $\bar{x}/L = [1 - (\Delta V_g^-/\Delta V_g^+)]^{-1}$ and $Q/e = \epsilon (\Delta V_g^- - \Delta V_g^+/(eL),$ where L is the SiO_2 thickness, e is the electronic charge, and ϵ is the static dielectric constant of SiO₂. These values of ΔV_g^+ and ΔV_g^- are for the average shifts between the curves in Figs. 1 and 2 and, along with the standard deviations indicated in the figure captions, were determined by computer analysis. For the data of these figures, the centroid and the number of trapped charges per unit area were determined from the photo I-V relations to be 33.1 \pm 0.5 nm and $(3.42 \pm 0.03) \times 10^{12} \text{ electrons/cm}^2$, respectively. The error of ± 0.5 nm in the centroid position, as determined by fitting the data from Figs. 1 and 2, indicates the power and accuracy of the photo I-V tech-

The photo *I-V* data were reproducible on any given sample. Displacement current effects, which were negligible, have been discussed in detail in recent publications

[5, 12]. Displacement currents can arise from additional charge trapping or from photodetrapping while the photo I-V measurements are being taken. Because of the low capture probability, which is $< 10^{-3}$ for sites related to the implanted Al discussed in the paper by Young et al. [8], charge trapping effects were negligible. Photodetrapping effects also were negligible (except in one case) for the energies used here (4.5 or 5 eV) and will be discussed later. Complete capacitance-voltage (C-V) curves were recorded before and after both the charging and the photo I-V measurements. Flat-band voltage shifts $\Delta V_{\rm FR}$ deduced from these C-V curves as shown in Fig. 3 were identical to the positive gate voltage bias photo I-V shift ΔV_g^+ to within a few tenths of a volt. This is consistent with a bulk trapped charge distribution, since C-V measurements are more sensitive than photo I-V measurements to charge at the Si-SiO₉ interface [5, 7].

• Experimental results

In Fig. 4, the centroid \bar{x} is plotted as a function of Al implant energy in the range of 15-40 keV for oxides with thicknesses of 49, 73, and 140 nm. The points in this figure connected by dashed lines were determined for the negative trapped charge from the photo I-V experimental technique. All samples in this figure were charged by avalanche injection from the Si substrate at current levels of 9×10^{-10} or 9×10^{-9} A [8]. The other lines are calculated for the implanted Al by using LSS theory [16]. Each experimental point in Fig. 3 represents the average of \bar{x} over many samples. Samples from the same wafer or different wafers processed months apart had centroid values for negative trapped charge that never differed by more than 2.5 nm. For all samples in Fig. 4, the fluence was 1×10^{13} Al/cm² and the post-implantation annealing was carried out at 1050°C for 30 min in N_o.

As seen in Fig. 4, there is some discrepancy between the experimental results and the LSS calculations for all energies and oxide thicknesses (the photo I-V results show the centroid position closer to the Al except for \bar{x} at 15 keV on the 73-nm and 140-nm samples). The rolloff and pinning of \bar{x} at the higher energy implants on the thinner oxide samples (for all energies on the 49-nm samples and for 30 and 40 keV on the 73-nm samples) are due to a significant fraction of the Al penetrating the Si substrate that is not sensed by the photo I-V technique. Otherwise, the data points should be independent of SiO, thickness. In addition to the pinning effect, the loss of Al to the Si reduces the trapping that is observed, as discussed in the companion paper by Young et al. [8]. The LSS theoretical plots also show deviations when Al is lost to the Si substrate, but this occurs at higher implantation energies than those shown in the experimental results. This discrepancy will be shown to be due to a broader ion distribution than that predicted theoretically.

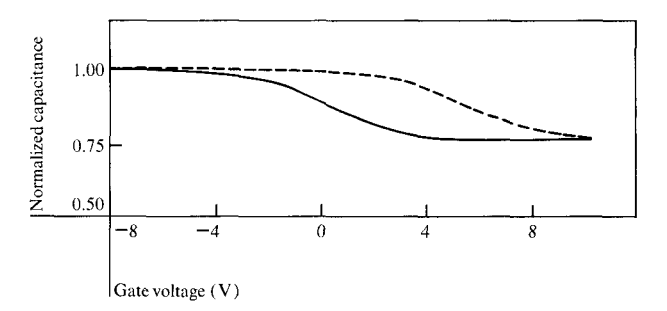


Figure 3 Normalized capacitance (total capacitance divided by the oxide capacitance) as a function of gate voltage. Samples are the same as in Fig. 1, the solid and dashed lines representing the control and charged samples, respectively. The flat-band voltage shift $\Delta V_{\rm FB}$ is 5.2 ± 0.1 V.

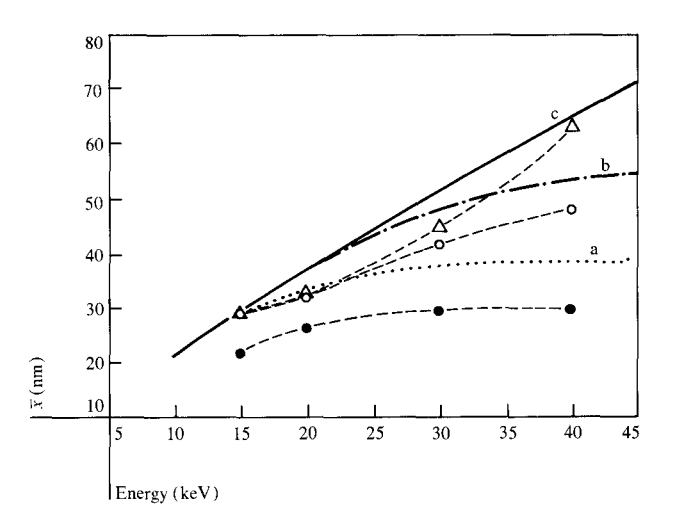


Figure 4 Values of \bar{x} as a function of Al implantation energy from 15–40 keV for SiO₂ layers 49, 73, and 140 nm thick. The points \bullet , \bigcirc , and Δ , respectively, are values for the trapped negative charge distribution using the photo *I-V* technique and the dashed lines connecting these points are visual aids only. The lines a, b, and c are the values predicted by LSS theory for the implanted Al distribution. All samples were charged by avalanche injection of electrons from the Si substrate.

The experimental conditions were varied to see what effect they had on the centroid position of the negative trapped charge. These centroids were found to be independent of the following experimental variables:

- 1. Amount of trapped charge—in the range from 10¹¹ to 10¹² electrons/cm².
- 2. Injection mechanism to fill traps—avalanche injection or internal photoemission from the Si substrate, or internal photoemission from the Al electrode; except for a small anomalous effect observed for the sample with a 40-keV implant into a 140-nm oxide, which will be discussed later.

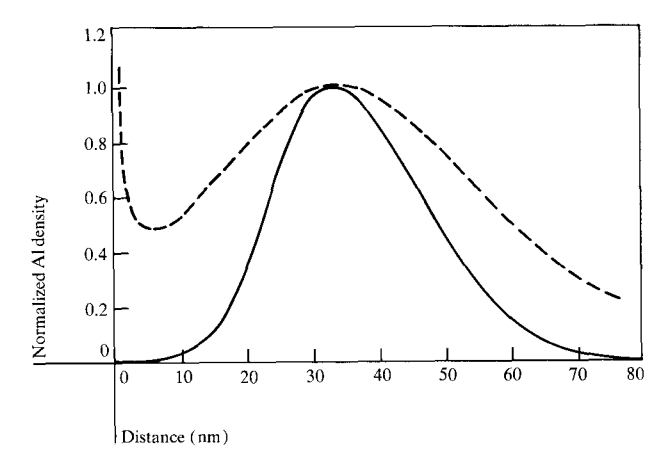


Figure 5 Normalized Al density for a 20-keV implant energy and a fluence of 1×10^{13} Al/cm² as a function of distance from the air-oxide interface into a SiO₂ film 77 nm thick. The normalization factor was the peak value of the Al density in the film. The dashed and solid lines are the profiles determined from SIMS measurements and LSS theory, respectively.

Table 1 Centroid comparison for a 20-keV Al implant into SiO₂.

Oxide thickness (nm)	Centroid (nm)		
	Photo I-V	SIMS	LSS
49	26.5	27.4 + 2.5	33.5
73	32.0	34.6 ± 2.5	36.7

- 3. Post-implant annealing conditions—from 600 to 1050°C for 30 min in N₂.
- 4. Fluence of Al—from 5×10^{12} to 2×10^{13} Al/cm².
- 5. Oxide thickness—in the range from 49-140 nm if the Al does not penetrate the Si substrate.

Items (1) and (4) were anticipated from the low capture probabilities (less than one out of every thousand electrons injected into the SiO₂ layer is captured) of the implanted Al-related trapping sites as discussed in Young et al. [8]. Item (3) was not expected. Since much more trapping under identical injection conditions was observed on the samples annealed at 600°C than on the samples annealed at 1050°C [8, 11], it was expected that part of the additional trapping would be caused by atomic displacement damage and would move the centroid toward the Al-SiO₂ interface. This was not the case. Annealing from 600 to 1050°C only removes some of the trapping sites surrounding the implanted Al distribution, as will be discussed next.

The photo *I-V* experiments presumably sensed negative charge trapped on sites related to the implanted Al. To confirm this experimentally and also profile the implanted Al distribution in the oxide layer, secondary ion mass spectroscopy (SIMS) was employed where the pri-

mary ion beam was O⁺ and a sputtering rate of approximately 0.2 nm/s was used on the SiO₂ layer. The samples were 77 nm of thermal SiO₂ on Si implanted with a fluence of 1×10^{13} Al/cm² at 20 keV. The SIMS measurements showed that the profile of the implanted Al was independent of post-implant annealing conditions (unannealed as compared with a 1050°C anneal in N_2 for 30 min). Figure 5 shows a profile of the implanted Al measured by SIMS and compares it to the profile calculated from LSS theory. Values of \bar{x} determined from the SIMS data of Fig. 5 are given in Table 1 for SiO_a layers 49 and 73 nm thick, and are compared with values determined from the photo I-V measurements and the LSS calculations. The centroids determined from the photo I-V and SIMS measurements are in good agreement for the two different oxide thicknesses. This implies that the distribution of the negative trapped charge (from photo I-V) is the same as that of the implanted Al (from SIMS). Figure 5 also shows that the full width at half maximum for the measured SIMS profile is approximately twice as large as that calculated from LSS theory. This is consistent with observations of Chu et al. for heavier ions at higher energies in thermal SiO₂ layers using He⁺ ion backscattering techniques [17, 18]. This broadening of the distribution implies that more Al should be lost to the Si substrate on thinner SiO₂ samples and that the measured values of \bar{x} should progressively deviate more with the LSS calculations as the oxide is made thinner. As mentioned previously, the former trend is seen in Fig. 4, where the rolloff due to Al penetration of the Si substrate is predicted by the LSS calculations to occur at somewhat higher implantation energies than observed experimentally. The latter trend is seen in Table 1 and in Fig. 4. In Fig. 4, the largest deviations with the LSS calculations for all energies occur on the 49-nm-thick SiO₂ samples (approximately 7-9 nm from 15-40 keV).

Attempts were made to photodetrap electrons trapped on the sites related to implanted Al with energies below the silicon dioxide conduction band edge in the range from 1-5.5 eV. As discussed in a previous publication [5], the gate and substrate were grounded and the internal field of the negative trapped charge was used to favor photodetrapping and block internal photoemission of electrons from the contacts at energies greater than 3 eV which would repopulate discharged trapping sites. Neither the full spectrum of a 900-W xenon high pressure lamp nor the spectrum of a 60-W deuterium lamp (which has a broad peak at approximately 5.5 eV) with a 5.5-eV low frequency pass filter (to prevent possible hole injection from the contacts and trapping) for times as long as hours was successful in removing many trapped electrons in any of the samples discussed here. In the most extreme case on the MOS structure with a 140-nm-thick SiO, layer and implanted at 40 keV, approximately 16 percent of the total number of trapped charges per unit area (2.9×10^{12}) electrons/cm²) was removed with the deuterium lamp. After the traps were initially charged by avalanche injection from the Si, \bar{x} for the charge removed was approximately 7 nm greater than that for the charge remaining. As mentioned earlier (see item 2-injection mechanism), only this sample (140-nm SiO₂, 40-keV implant) showed a pronounced dependence of the centroid position on injection mechanism. The \bar{x} value decreased by approximately 12.5 nm when photoinjection from the Al-SiO, interface with 4.5-eV light was used to fill traps; this result was independent of the number of trapped charges per unit area in the range from 1×10^{11} to 1×10^{12} electrons/cm². These two experimental observations are consistent with each other and imply that photodetrapping can explain the anomaly mentioned in item 2. This photodetrapping was observed to be influenced by the local fields [3, 4, 19] and optical interference patterns [19] and/or the light energy in the SiO_2 layer since values for \bar{x} measured by the photo I-V technique varied somewhat under photoinjection conditions (injecting interface and light wavelengths used).

Discussion of results

Our results cannot be compared readily with those of Johnson et al. [1] (Al implanted at 20 keV with a fluence of 10¹⁴ Al/cm² into a SiO₂ layer 140 nm thick), since most of their measurements and analysis of flat-band voltages and photocurrents were on unannealed MOS structures. They deduced a centroid for trapped space charge injected from the Si-SiO₂ interface at 67 nm from the Al-SiO₂ interface and observed that this space charge could be photodetrapped at energies greater than or equal to 4 eV. They correctly concluded that the centroid was in deeper from the Al-SiO, interface than expected because every injected electron from the Si-SiO, interface was captured (capture probability of unity). This favors charge buildup near the injecting interface. They also concluded that a substantial fraction of the electron traps were due to displacement damage. Our use of high temperature annealing treatments and lower fluences avoided the problems encountered by Johnson et al. [1].

In summary, the centroid of electrons trapped in the SiO, layer of an MOS structure resulting from aluminum implantation has been located by the photo *I-V* technique. This centroid is essentially identical to those of the implanted Al as determined by SIMS measurements and independent of annealing temperature from 600-1050°C. Comparisons of centroids from photo I-V and SIMS measurements for different oxide thicknesses imply that the distributions are also identical. For implantation energies from 15-40 keV, the centroids were found to be in fair agreement with those predicted by the LSS calculations of Gibbons, Johnson, and Mylroie [16].

Acknowledgments

The authors acknowledge the critical reading of this manuscript by M. I. Nathan and A. B. Fowler and helpful discussions with B. L. Crowder and J. F. Ziegler. The SIMS measurements were performed by F. W. Anderson and J. C. Webber of the IBM East Fishkill facility. The thermal oxide layers were grown by J. A. Kucza, E. J. Petrillo, and H. F. Lazzarri. The thin Al electrodes were deposited by E. D. Alley, and H. Ripke provided continuing experimental assistance.

This research was supported in part by the Defense Advanced Research Projects Agency, U.S. Department of Defense, and was monitored by the Deputy for Electronic Technology (RADC) under Contract No. F19628-76-C-0249.

References

- 1. N. M. Johnson, W. C. Johnson, and M. A. Lampert, J. Appl. Phys. 46, 1216 (1975).
- 2. B. H. Yun, Appl. Phys. Lett. 25, 340 (1974).
- 3. P. C. Arnett and B. H. Yun, Appl. Phys. Lett. 26, 94 (1975).
- 4. P. C. Arnett, J. Appl. Phys. 46, 5236 (1975).
- 5. D. J. DiMaria, J. Appl. Phys. 47, 4073 (1976)
- 6. A. S. Grove, Physics and Technology of Semiconductor Devices, John Wiley & Sons, Inc., New York, 1967, Ch. 9.
- 7. R. J. Powell and C. N. Berglund, J. Appl. Phys. 42, 4390 (1971).
- 8. D. R. Young, D. J. DiMaria, W. R. Hunter, and C. M. Serrano, IBM J. Res. Develop. 22, 285 (1978, this issue).
- 9. E. H. Nicollian, A. Goetzberger, and C. N. Berglund, Appl. Phys. Lett. 15, 174 (1969); E. H. Nicollian and C. N. Berglund, J. Appl. Phys. 41, 3052 (1970).
- 10. B. E. Deal, E. H. Snow, and C. A. Mead, J. Phys. Chem. Solids 27, 1973 (1966).
- 11. D. R. Young, D. J. DiMaria, and W. R. Hunter, J. Electron. Mater. 6, 569 (1977).
- 12. D. J. DiMaria, Z. A. Weinberg, and J. M. Aitken, J. Appl. Phys. 48, 898 (1977).
- 13. J. M. Aitken, D. J. DiMaria, and D. R. Young, IEEE Trans. Nucl. Sci. NS-23, 1526 (1976).
- 14. D. J. DiMaria, Z. A. Weinberg, J. M. Aitken, and D. R. Young, J. Electron. Mater. 6, 207 (1977).
- 15. D. J. DiMaria, J. Appl. Phys. 45, 5454 (1974)
- 16. J. F. Gibbons, W. S. Johnson, and S. W. Mylroie, Projected Range Statistics of Semiconductors and Related Materials, 2nd ed., Halstead Press, John Wiley & Sons, Inc., New York, 1975. In our calculations, we corrected for the difference in density between single-crystal quartz (listed in the tables) and the thermal SiO₂ studied here. This ratio (thermal SiO₂ density to single-crystal quartz density) was 0.84. Also, we have included the third moment corrections which give the calculated profiles the skewed shape shown in Fig. 5
- 17. W. K. Chu, B. L. Crowder, J. W. Mayer, and J. F. Ziegler, Appl. Phys. Lett. 22, 490 (1973).
- 18. W. K. Chu, B. L. Crowder, J. W. Mayer, and J. F. Ziegler, Ion Implantation in Semiconductors and Other Materials. B. L. Crowder, ed., Plenum Press, New York, 1973, p. 225.
- 19. D. J. DiMaria and P. C. Arnett, IBM J. Res. Develop. 21, 227 (1977).

Received October 14, 1977

The authors are located at the IBM Thomas J. Watson Research Center, Yorktown Heights, New York 10598.